Journal of Power Sources 267 (2014) 160–170

Contents lists available at ScienceDirect

Journal of Power Sources

journal homepage: www.elsevier.com/locate/jpowsour

In situ mapping of potential transients during start-up and shut-down of a polymer electrolyte membrane fuel cell

E. Brightman*, G. Hinds

National Physical Laboratory, Teddington, Middlesex TW11 0LW, United Kingdom

HIGHLIGHTS

- A unique reference electrode array allows mapping of electrode potential in a PEMFC.
- Potential mapping and CO_2 measurement were used simultaneously for the first time.
- Drier conditions led to less corrosion; evidence links this to membrane resistivity.
- Most severe carbon loss located near outlet for start-up and inlet for shut-down.
- Results provide new insights into reverse current decay mechanism.

ARTICLE INFO

Article history:
Received 18 November 2013
Received in revised form
7 May 2014
Accepted 10 May 2014
Available online 24 May 2014

Keywords:
Polymer electrolyte membrane fuel cell
Start-up/shut-down
Reference electrode
Carbon corrosion

ABSTRACT

Progression of a fuel/air front through the anode flow-field during start-up or shut-down of a polymer electrolyte membrane fuel cell is known to generate elevated cathode potentials, leading to corrosion of the carbon catalyst support. Here we present spatially resolved measurements of such potential transients in an operating fuel cell, using an innovative reference electrode array combined with quantification of carbon corrosion by measurement of CO_2 in the cathode outlet. A systematic study of the effect of relative humidity on start-up/shut-down potential transients and carbon corrosion rates was carried out at open circuit and with the application of a small external load. The results are discussed in the context of a schematic framework for the reverse current decay mechanism expressed in terms of local electrode potential. In all cases carbon corrosion was more severe during start-up than during shut-down, with the highest cathode potentials measured opposite the anode outlet during start-up and opposite the anode inlet during shut-down. The carbon corrosion rate was least severe under the driest conditions, which was attributed to the increased membrane resistivity. This new technique provides a powerful diagnostic tool for evaluation of start-up/shut-down tolerant catalyst layers and optimisation of fuel cell hardware design.

1. Introduction

Polymer electrolyte membrane fuel cells (PEMFCs) are a pivotal technology for a future hydrogen economy. However, widespread commercialisation is currently hindered by high cost and limited durability of components. One of the major PEMFC degradation modes occurs during start-up and shut-down (SU/SD), whereby high transient cathode potentials due to the presence of a hydrogen/air front in the anode flow-field lead to corrosion of the carbon-based catalyst support [1]. Repetitive SU/SD events can result in dramatic loss of performance arising from a decrease in active catalyst area [1,2]. There has been a great deal of academic and commercial interest in this degradation mechanism in recent years, as it is a particularly important factor in automotive systems where many start/stop cycles can be expected, and where space and cost limitations prevent the use of a nitrogen purge or similar mitigation strategy. A recent review by Yu et al. [3] summarises much of the research that has been carried out in this area, and highlights the difficulty of measuring the potential transients in situ. Lamibrac et al. [4] used a specially designed segmented cell to measure the transient local current densities arising from the start-up process in order to estimate the amount of carbon corrosion from the charge exchanged. They found that the segments of the cell that were exposed to air for the longest were

* Corresponding author. Tel.: +44 208 943 8564.
E-mail address: edward.brightman@npl.co.uk (E. Brightman).

http://dx.doi.org/10.1016/j.jpowsour.2014.05.040
0378-7753/

most degraded by carbon corrosion. Several researchers have made measurements of CO_2 in the cathode gas stream in order to quantify the extent of carbon corrosion. Linse et al. [5] used an infrared analyser to monitor the concentration of CO_2 in the cathode outlet with a known flow rate, which enabled them to calculate the amount of carbon corrosion occurring under a range of systematically controlled conditions. They showed that under open circuit conditions the carbon corrosion rate was proportional to the gas front residence time and that with an external load carbon corrosion was suppressed (more effectively for shut-down than for start-up). They also observed an approximately linear dependence of the rate of carbon corrosion on relative humidity (RH). However, they were unable to measure the local cathode potential in their experiments. Kreitmeier et al. [6] used mass spectrometry to measure CO_2 concentration, and constructed a cell comprising linear parallel channels with 11 gas extraction ports located along the length of the flow-field. They found that carbon loss from start/stop cycling was most severe towards the outlet, with regions in the middle of the flow-field being least affected. Comparison of rates of carbon corrosion during start-up and shut-down using such methods has revealed contradictory results, with some authors reporting that carbon corrosion is more severe during start-up than shut-down [6,7] and others the opposite [5]. This discrepancy has been attributed to the competing effects of Pt hydride/oxide redox reactions and the differing diffusion coefficients of H_2 and O_2/N_2 [6].

Whilst measurement of evolved CO_2 has proved extremely useful in elucidating the effects of SU/SD cycling on PEMFCs, there have been limited attempts to measure the cathode potential during start/stop events, mainly due to the practical limitations of using reference electrodes in PEMFCs. For example, Shen et al. [8] used a customised membrane electrode assembly (MEA) with a hydrogen reference electrode located on the membrane adjacent to the edge of the active area of the MEA to measure the electrode potentials, together with copper wires sandwiched between two membranes to measure the membrane potential. An interfacial potential difference between cathode and membrane as high as 1.6 V was indicated by the authors, although use of the copper reference electrodes was not subject to a rigorous calibration procedure.

A novel fuel cell reference electrode has been developed at the National Physical Laboratory (NPL) that overcomes the limitations of conventional fuel cell electrodes by making contact with the working electrode through the back of the gas diffusion layer (GDL) [9]. Very small diameter Nafion tubing is inserted through the end plates of the fuel cell to act as a salt bridge, and the ionic pathway is extended through the GDL to the electrode by impregnating the GDL with Nafion at the point of contact. This innovative configuration ensures that potential drop effects in the membrane and electrode edge effects are avoided, and by using an array of such electrodes the spatial distribution of electrode potential can be measured. The reference electrode is relatively straightforward to implement on a technical-scale cell and can therefore provide in situ measurements on a commercial prototype with minimal perturbation of the system.

In the present study, the NPL reference electrode array has been applied to a generic research cell, in parallel with measurement of CO_2 in the cathode outlet stream, to investigate the effect of relative humidity on the potential transient and concomitant carbon oxidation under SU/SD cycling, with spatial resolution of the potential transient and quantification of the total carbon oxidation. SU/SD cycles were carried out under open circuit conditions and in the presence of an external fixed load on the cell, which is a commonly used mitigation strategy. An alternative mitigation strategy, whereby Nafion tubing was used in an attempt to enhance the lateral proton conductivity between affected regions at the cathode, was also investigated.

2. Reverse current decay mechanism

The reverse current decay mechanism first proposed by researchers at UTC Fuel Cells [1] is generally accepted to be responsible for the loss of performance observed as a result of SU/SD cycling. Although the general basis of the mechanism appears sound, discussion in the literature is not ideal, focusing on parameters such as electrolyte potential that cannot physically be measured. In our opinion, electrode potential is a more appropriate basis for construction of a SU/SD scheme as it can be verified by measurement. Division of the active area of the PEMFC into four regions during SU/SD is shown schematically in Fig. 1. Before start-up of a PEMFC, both anode and cathode compartments are filled with air, either due to an air purge or via gradual leakage from the atmosphere through the anode seal or across the membrane from the cathode. During start-up (Fig. 1a), hydrogen entering the anode flow-field leads to generation of excess protons and electrons close to the anode inlet (Region 1) with an electrode potential close to that of the reversible hydrogen electrode (~0 V). In Region 2, the electrode potential remains close to the open circuit potential for oxygen/water on Pt (~1 V). If the anode is considered in isolation, under these conditions a mixed potential will be established between Region 1 and Region 2, depending on the polarisation of each reaction (in this case the oxygen reduction reaction will show greater polarisation) and the ionic conductivity of the electrolyte phase. Although there is high electronic conductivity throughout the anode (between Region 1 and Region 2) the lateral proton conductivity is relatively low. Therefore the electrode potential in each region will be polarised only slightly towards that of the other region due to the large ohmic drop in the ionic phase. Representative values based on those observed in this work are given in Fig. 1.

Prior to start-up, the electrode potential at the cathode is at the open circuit potential for oxygen/water on Pt (~1 V), which is a mixed potential determined by the balance between the water oxidation/oxygen reduction redox reaction and the platinum hydride/oxide reactions. When hydrogen enters the anode compartment, excess protons and electrons are generated in the anode catalyst layer (Region 1). Normally, these protons can only cross the membrane to Region 3 to be consumed in the oxygen reduction reaction if there is an electronically conducting path to simultaneously supply the electrons from Region 1, a condition that is not satisfied at open circuit. Similarly, although the electrons generated in Region 1 can readily move to Region 2, the low lateral proton conductivity in the electrolyte phase limits the oxygen reduction reaction in Region 2. The simultaneous demand for electrons in Region 3 and protons in Region 2 provides the driving force for an oxidation reaction to occur in Region 4. Oxidation of water, carbon or platinum is possible, which provides a complete circuit consisting of lateral electronic current in each electrode and through-plane proton current in the membrane. As a result the cathode potential in Region 4 is shifted to more positive potentials (typically > 1.4 V) to generate the required protons and electrons. The cathode potential in Region 3 and the anode potential in Region 2 are both shifted to more negative potentials to support the oxygen reduction reaction, which is the rate limiting step of the process due to its relatively slow kinetics compared to hydrogen oxidation.

The reverse process occurs during shut-down, the main difference being that air is displacing hydrogen rather than vice versa. In this case the potential map of the active area is a mirror image of that during start-up and it is the cathode potential in Region 3 that

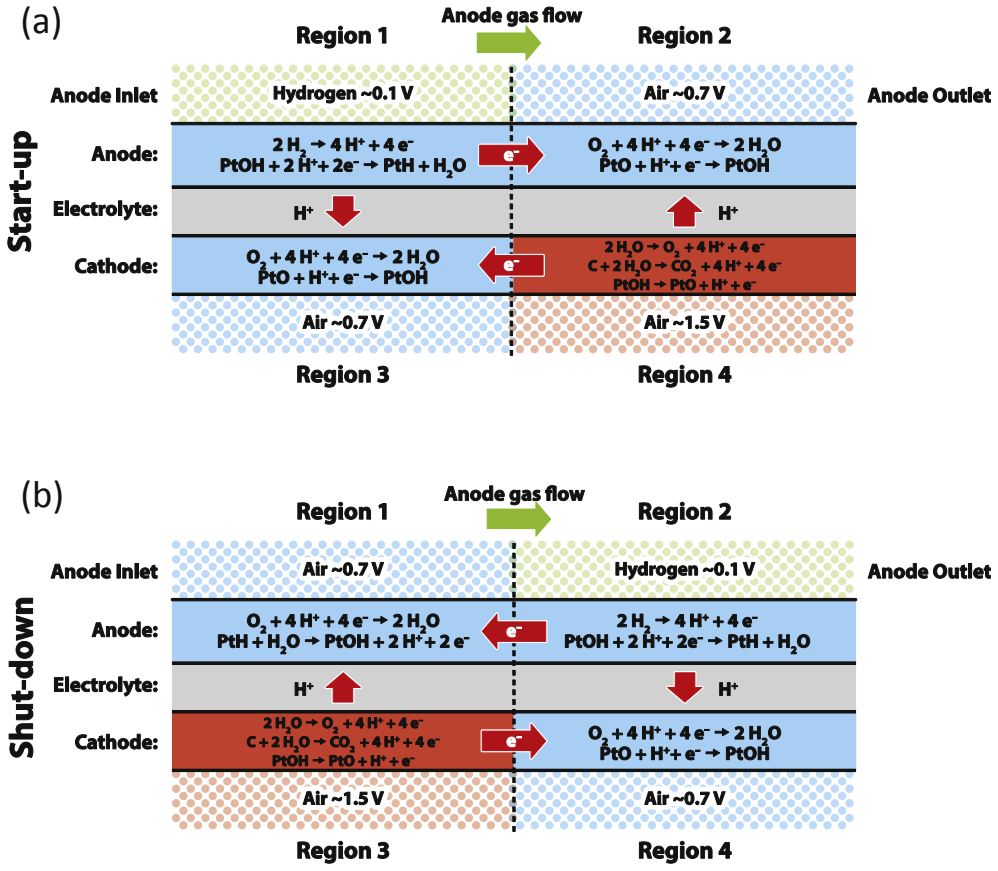

Fig. 1. Schematic diagram illustrating the principle of the reverse current decay mechanism.

is driven to more positive potentials (Fig. 1b). However, differing behaviour during start-up and shut-down can be observed depending on platinum oxide and gas displacement effects, the relative strength of which can vary depending on parameters such as Pt loading, gas flow rate and flow-field design.

The influence of platinum hydride/oxide redox reactions on carbon support corrosion during SU/SD is included in the schematic diagrams in Fig. 1. During start-up, when hydrogen flows onto the oxidised platinum surface in Region 1 (Fig. 1a) reduction of the platinum oxide consumes protons and electrons, which tends to decrease the rate of supply to Region 3 and Region 2 respectively and slow down the rate of carbon corrosion in Region 4. Similarly, during shut-down when air flows onto the reduced platinum surface in Region 1 (Fig. 1b), oxidation of the platinum generates protons that can be used to supply the oxygen reduction reaction in Region 1, decreasing the need for protons to be supplied from the carbon corrosion reaction in Region 3 and thereby reducing the rate of carbon corrosion. Thus, in general the effect of the platinum hydride/oxide kinetics is to mitigate carbon corrosion. The main difference between start-up and shut-down is observed in the air-filled region on the anode, where oxygen reduction occurs, which as previously mentioned is the rate limiting step for the process. During start-up the platinum oxide surface in Region 2 of Fig. 1a is reduced due to the more negative transient potential, which provides an increased driving force for the carbon oxidation reaction in Region 4. In contrast, during shut-down the reduced platinum surface in Region 1 of Fig. 1b is oxidised, generating additional protons and electrons for the oxygen reduction reaction in this region and thereby decreasing the driving force for carbon oxidation in Region 3.

Mitigation strategies for SU/SD degradation generally fall into two categories: engineering and materials solutions. Engineering solutions include purging with an inert gas, use of high flow rates and/or application of a small electrical load to the cell during the SU/SD process. The use of an external load effectively short-circuits the lateral flow of electronic current in each electrode and reduces the extent of undesirable polarisation of the cathode. In principle, according to the scheme outlined in Fig. 1, short-circuiting the proton conducting phase would also have an equivalent mitigating effect, although in practice this is more challenging due to the high through-plane proton conductivity of the ionomer phase. The effectiveness of both of these strategies is explored in this work. Materials solutions include the use of a low platinum loading on the anode to limit the rate of oxygen reduction [10], development of more corrosion resistant carbon support materials [11] and incorporation of oxygen evolution reaction catalysts into the cathode to promote water oxidation over carbon oxidation [12]. The choice of mitigation strategy depends strongly on the application and cost/benefit analysis.

The SU/SD process is commonly represented in the literature by a dual cell configuration consisting of a fuel cell in parallel with an electrolyser. Measurements in dual cell configuration have reproduced the carbon corrosion observed in single cells [1], but the extent to which such measurements are fully representative of a real fuel cell depends on the validity of the assumption of zero lateral proton conductivity in the electrodes. The NPL reference electrode array makes possible for the first time in situ mapping of potential transients across the active area of both electrodes in a real single cell during the SU/SD process, allowing validation of the four region scheme presented in Fig. 1.

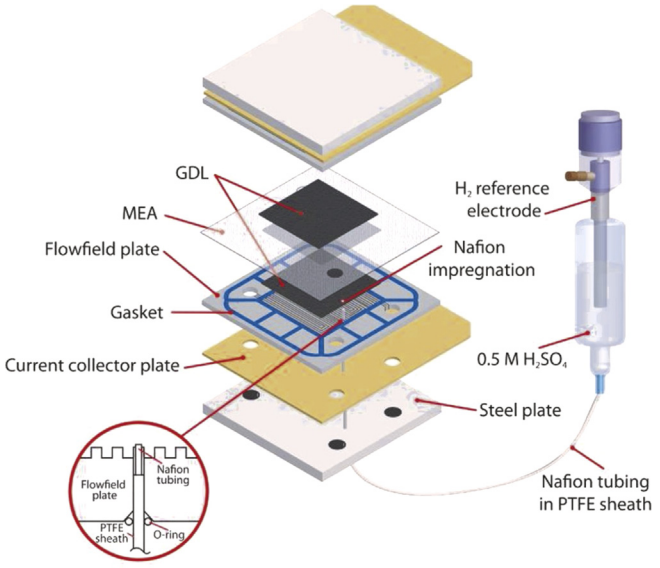

Fig. 2. Schematic diagram of a single NPL through-plate reference electrode. Inset: hole in graphite flow-plate and O-ring sealing arrangement.

3. Experimental

The NPL through-plate reference electrode has been described previously [9] and is illustrated in Fig. 2. It consists of fine Nafion tubing (Perma Pure, NJ, USA) with 0.64 mm ID and 0.84 mm OD enclosed in a polytetrafluoroethylene (PTFE) sheath of 1.01 mm ID and 1.27 mm OD (Adtech Engineering Ltd., UK), which is filled with deionised water to ensure maximal proton conductivity of the Nafion. This acts as a salt bridge and is inserted into a glass vessel containing 0.5 M H_2SO_4, into which is placed a Hydroflex hydrogen reference electrode (Gaskatel GmbH, Germany). The other end of the Nafion tubing is inserted through a hole in the end plates of the cell and sealed using an O-ring as illustrated in the inset in Fig. 2. In order to create an ion-conducting path through the GDL, the GDL is impregnated with Nafion at the point of contact with the salt bridge using a 2 μL pipette to dispense a 50:50 mixture of 10% Nafion dispersion in water (Sigma Aldrich, UK) and 2,2,3,3-tetrafluoro-1-propanol (Sigma Aldrich, UK). This creates a circular region of ionic conductivity through the GDL approximately 3 mm in diameter. An array of nine reference electrodes was used in order to map the spatial distribution of the electrode potential. The locations of the points of contact with respect to the serpentine flow-field are shown in Fig. 3.

A 7 cm × 7 cm single cell PEMFC was used for all measurements with MEAs supplied by Johnson Matthey Fuel Cells Ltd (JMFC, UK). The MEAs consisted of a perfluorosulfonic acid membrane and Pt/C electrodes with Pt loadings of 0.38 mg cm^{-2} (cathode) and 0.07 mg cm^{-2} (anode). A fresh MEA was used for the tests at each relative humidity (RH) level. A six parallel channel serpentine impregnated graphite flow-field with 1 mm × 1 mm channel cross-section was used on both anode and cathode in partial counter-flow mode. Experiments were carried out using a Hydrogenics FCATS-G50 test stand, with compression of the cell achieved using a pressurised gas/piston arrangement with a compression pressure

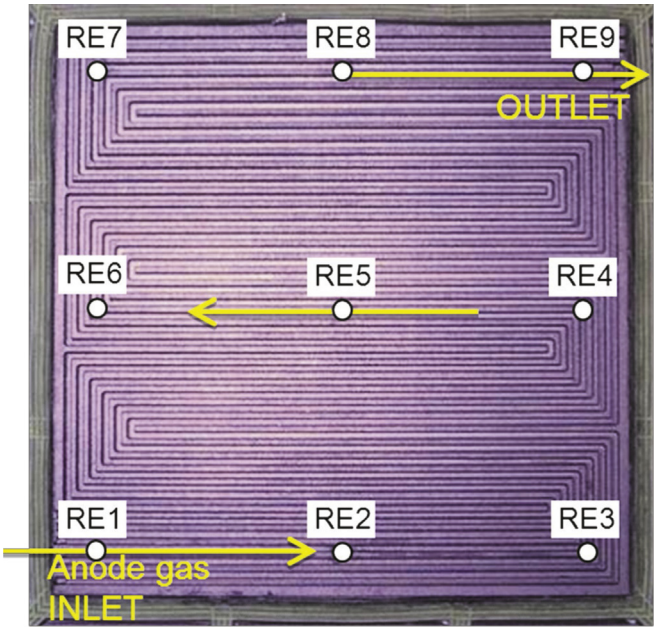

Fig. 3. Anode flow-field showing positions of nine reference electrodes (RE), which are placed on the cathode side, relative to the anode gas flow direction.

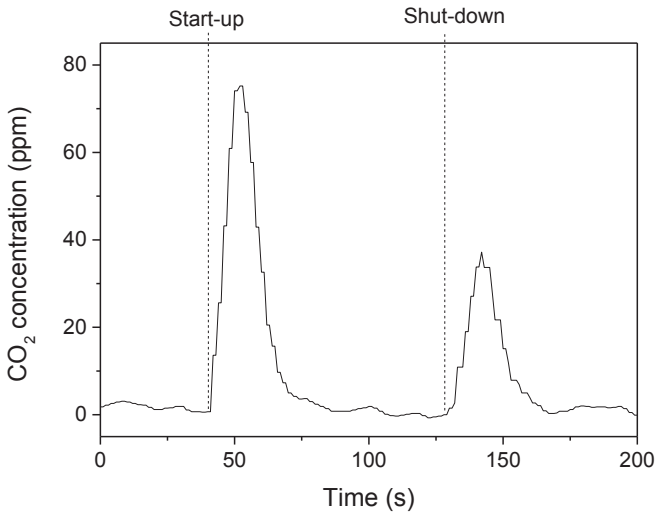

Fig. 4. CO_2 concentration measured at the cathode outlet for a single SU/SD cycle at 100% RH.

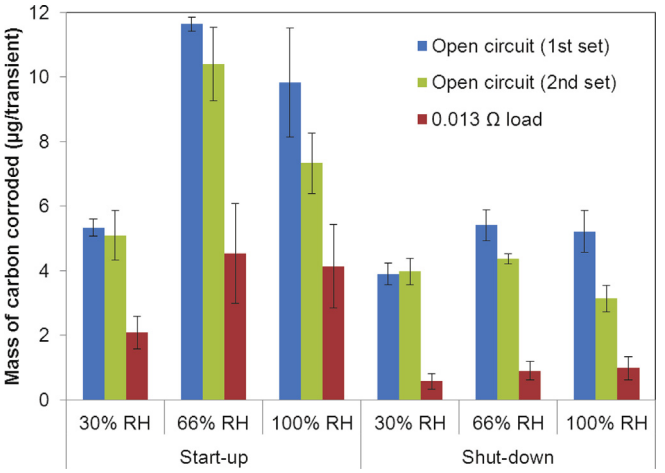

Fig. 5. Amount of carbon corrosion calculated from measured CO_2 concentration in cathode outlet gas stream.

of 7 barg. The MEAs were pre-conditioned at 80 °C and 100% RH at a constant current density of 0.5 A cm^{-2} for 18 h at an outlet pressure of 3 barg. The SU/SD testing was carried out at atmospheric outlet pressure, with a constant cell temperature of 80 °C. The cathode side of the cell was supplied with zero grade air containing <1 ppm CO_2 (BOC Ltd, UK), whilst the anode side was fitted with a Swagelok 40-series manual 4-way crossover valve enabling rapid switching between zero grade air and pure H_2. The use of a crossover switching valve avoided any fluctuations in gas flow rate when switching. The cathode outlet gas stream was connected to a condenser and water trap before passing through an in-line infrared GMP343 CO_2 probe (Vaisala Oyj., Finland) connected to a PC. The electrode potentials were measured on a NI-9205 32-channel analogue input module in a compactDAQ chassis (National Instruments, USA), which was controlled by a LabVIEW program that simultaneously logged the nine electrode potentials, cell potential, and the CO_2 concentration.

In this study, humidifier temperatures of 52.5°C ± 0.5 °C, 70°C ± 0.5 °C and 80 °C ± 0.5 °C were used, corresponding to RH values of 30 ± 4% (MEA#1), 66 ± 2% (MEA#2) and 100 ± 2% (MEA#3) respectively. After conditioning, the cell was purged with nitrogen at 2 sL min^{-1} for 1 h before switching to air fed to both sides of the cell for the start of the experiments. The flow rate of air on the cathode was held constant at 1.0 sL min^{-1} throughout the experiments, whilst the hydrogen and air fed to the anode were both supplied at a nominal (dry) flow rate of 0.2 sL min^{-1}. Additional SU/SD experiments were carried out at anode flow rates of 0.6 sL min^{-1} and 0.1 sL min^{-1} on MEA#1 at 66% RH. SU/SD cycles were carried out by manually switching the crossover valve at 90 s intervals. In order to obtain a reliable dataset, SU/SD cycling was repeated 5 times at open circuit, followed by 10 times under external load conditions, and finally 5 more times at open circuit. The CO_2 concentration in the cathode outlet gas stream was found to take approximately 60 s to return to its baseline level.

For the application of the external load, the load bank of the Hydrogenics test stand was used under manual control in constant resistance mode to apply a resistance of 0.013 Ω, (i.e. 0.637 Ω cm^2) which was the minimum value available in this mode, and the current was measured using a Fluke 365 clamp meter (Fluke Corporation, USA). The load was connected throughout, and a SU or SD event was defined as switching on or off the supply of hydrogen to the cell. An analogous mitigation strategy involving short-circuiting

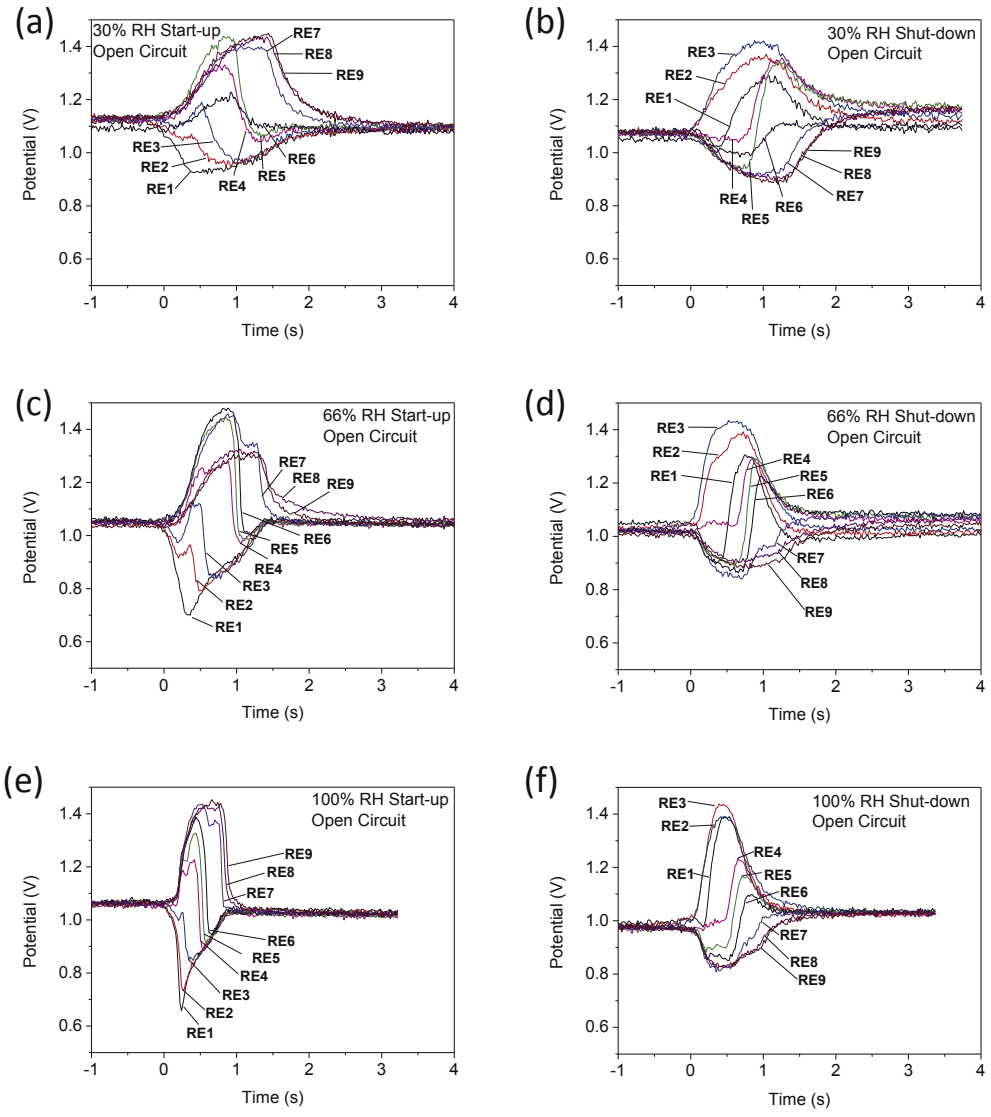

Fig. 6. Cathode potential transients as a function of flow-field location during start-up/shut-down at open circuit.

of the cathode ionomer phase between inlet and outlet was explored by connecting the locations of RE1 and RE9 with hydrated Nafion tubing to investigate whether this would have any beneficial effect on the rate of carbon corrosion.

4. Results and discussion

4.1. CO_2 measurements

Measurements of CO_2 concentration in the cathode outlet as a function of time showed a distinct spike in concentration corresponding to each SU/SD event, as shown for a typical SU/SD cycle at 100% RH in Fig. 4. The amount of carbon corrosion during each event was estimated by integration of each spike. The results plotted in Fig. 5 show the average and standard deviation of the first 5 SU/SD cycles carried out at open circuit, 10 cycles under external load, and a further 5 cycles at open circuit. In all cases, the amount of carbon corrosion observed was significantly higher during start-up than during shut-down, a trend that was most evident at 66% RH and 100% RH. The more severe carbon corrosion observed during start-up compared with shut-down at open circuit is consistent with the majority of observations in the literature [6,7], although an opposite trend has been reported in isolated cases [5], which highlights the importance of taking into account individual design factors such as flow-field geometry, gas permeability, Pt loading and mode of operation.

For both start-up and shut-down, carbon corrosion was least severe under the driest set of conditions (30% RH), which would be expected due to the participation of water in the carbon oxidation reaction and the dependence of ionomer conductivity on RH. This is also reflected in the level of background degradation that occurred over the course of each experiment, with a fresh MEA used at each RH level. The magnitude of the drop in average carbon corrosion rate between the first 5 SU/SD cycles and the last 5 SU/SD cycles increases with RH level. The decrease in carbon corrosion rate on increasing RH from 66% to 100% may be ascribed to the reduced residence time (which will be discussed further in the next section) and possibly also localised flooding, which would reduce the area of the anode that is exposed to air. This latter conclusion is supported by the more significant drop in corrosion rate in the second set of open circuit measurements at 100% RH for this MEA, since the flow of current during the "on" state would lead to further water formation at the cathode. A similar result was obtained by Linse et al. [5] who supported this conclusion with the observation that CO_2 evolution during consecutive transients became highly irregular, which was also the case in the present study.

As expected, with the application of an external load, the CO_2 measurements demonstrate a significant mitigation of carbon corrosion under all conditions tested. The effect of the external load was more significant during shut-down than during start-up, which may be explained by the more rapid kinetics of hydrogen oxidation compared to oxygen reduction, since during shut-down displacement of the hydrogen by air is accelerated by additional oxidation of hydrogen due to the external load. No significant effect of connecting Nafion salt bridges between locations RE1 and RE9 on the cathode flow-field was observed on the carbon corrosion rate. In principle, if the ionic conductivity between these two locations could be increased sufficiently, mitigation of carbon corrosion could be achieved but clearly the conductivity of the Nafion tubing is limiting in the present case.

4.2. Potential transients

Representative cathode potential transients during SU/SD at open circuit are plotted in Fig. 6, showing the potential measured against each of the nine reference electrodes. Videos of the potential transients in a 3 × 3 arrangement representative of the location of the measurement within the flow-field are available in Supplementary information of the online version of this paper. Transient spikes in potential on the cathode (up to 1.48 V) are observed in regions opposite to which air is present at the anode. These correspond to the locations at which the most severe carbon corrosion occurs, i.e. near the anode outlet during start-up and near the anode inlet during shut-down, as illustrated in Fig. 7. Away from these regions, the cathode potential drops below the open circuit value of ~1 V due to the cathodic reaction (oxygen reduction) opposite the hydrogen-filled section of the anode (i.e. Region 3 in Fig. 1a for SU and Region 4 in Fig. 1b for SD). As observed in a preliminary study [9], during start-up this negative shift in potential is relatively localised opposite the anode inlet, rather than tracking the fuel/air boundary as it moves through the anode flow-field. There is some limited extension of Region 1 in Fig. 1a to the middle of the flow-field under fully-humidified conditions, but at much less negative potentials. Otherwise Region 1 is confined to the inlet channel, which confirms the perspective that the largest driving force for the effect exists between regions with a high spatial separation due to the low lateral proton conductivity in the electrode. It also challenges the assumption made in models in the literature that the cathode potential changes abruptly opposite the air/fuel boundary [7].

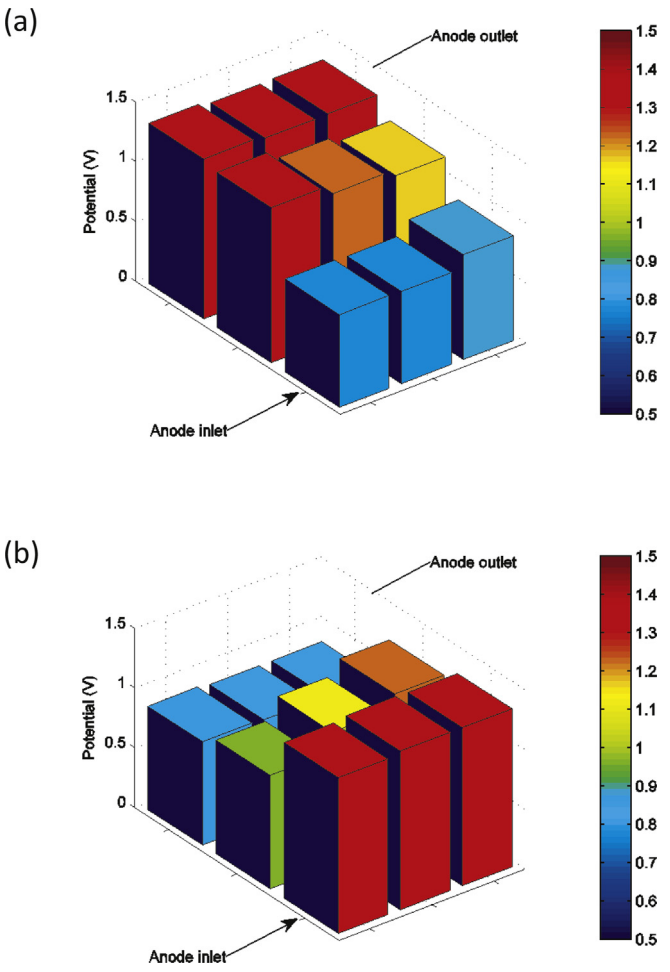

Fig. 7. Snapshots of the cathode potential during (a) start-up and (b) shut-down at 100% RH, open-circuit mode, plotted in 3 × 3 formation representative of the location of the measurement points on the fuel cell active area.

Supplementary Videos related to this article can be found online at http://dx.doi.org/10.1016/j.jpowsour.2014.05.040.

Representative cathode potential transients during SU/SD with the application of an external load of 0.013 Ω are plotted in Fig. 8, and the key features of the potential transients shown in Figs. 6 and 8 are summarised in Fig. 9. The results obtained using an external load will be discussed shortly, after an analysis of the summary data in Fig. 9. It is evident that the duration of the potential transients decreases with increasing RH for both start-up and shut-down (Fig. 9a). The reason for this is that the mass flow controllers were calibrated for dry gas, and subsequently adding water vapour to the gas stream leads to an increase in volume. There is also an increase in the volumetric flow rate through the cell at 80 °C by a factor of 1.29 assuming ideal gas behaviour (compared to the set-point which is calibrated at 0 °C). Table 1 gives the calculated humidified volume of 1 L of dry gas at 80 °C and the calculated flow rates based on a set-point of 0.2 sL min^{-1} for each humidity setting, using the formulae of Hardy [13]. The difference between the calculated results for hydrogen and those for air is negligible within the variability of the test stand temperature and flow rate control systems. The six parallel serpentine channels in the flow field each have a length of 490 mm and cross sectional area of approximately 1 mm^2, forming a total volume of 2940 mm^3. Therefore the minimum time taken for the gas front to sweep through the flow-field is 0.59 s at 30% RH, 0.48 s at 66% RH and 0.36 s at 100% RH, and these values are indicated on Fig. 9a. Clearly, the potential data show that a H_2/air front persists for considerably longer than this (by a factor of around 3), which is due to inefficient displacement of gas in the additional volume associated with the porosity of the GDL and anode catalyst layer.

It is therefore important to take into account the effect of residence time of the fuel/air front in the analysis of potential transients at different RH levels. Despite the longer residence time of the gas front under dry conditions, SU/SD transients at 30% RH caused the lowest amount of carbon corrosion under the conditions studied. At open circuit, the maximum potential observed at the cathode does not vary significantly with RH during either start-up or shut-down (Fig. 9b). In contrast, the minimum potential observed at the cathode decreases significantly with increasing humidity (Fig. 9c), indicating a correspondingly higher oxygen reduction current in Region 3 during start-up and in Region 4 during shut-down. The observed trend in CO_2 evolution with

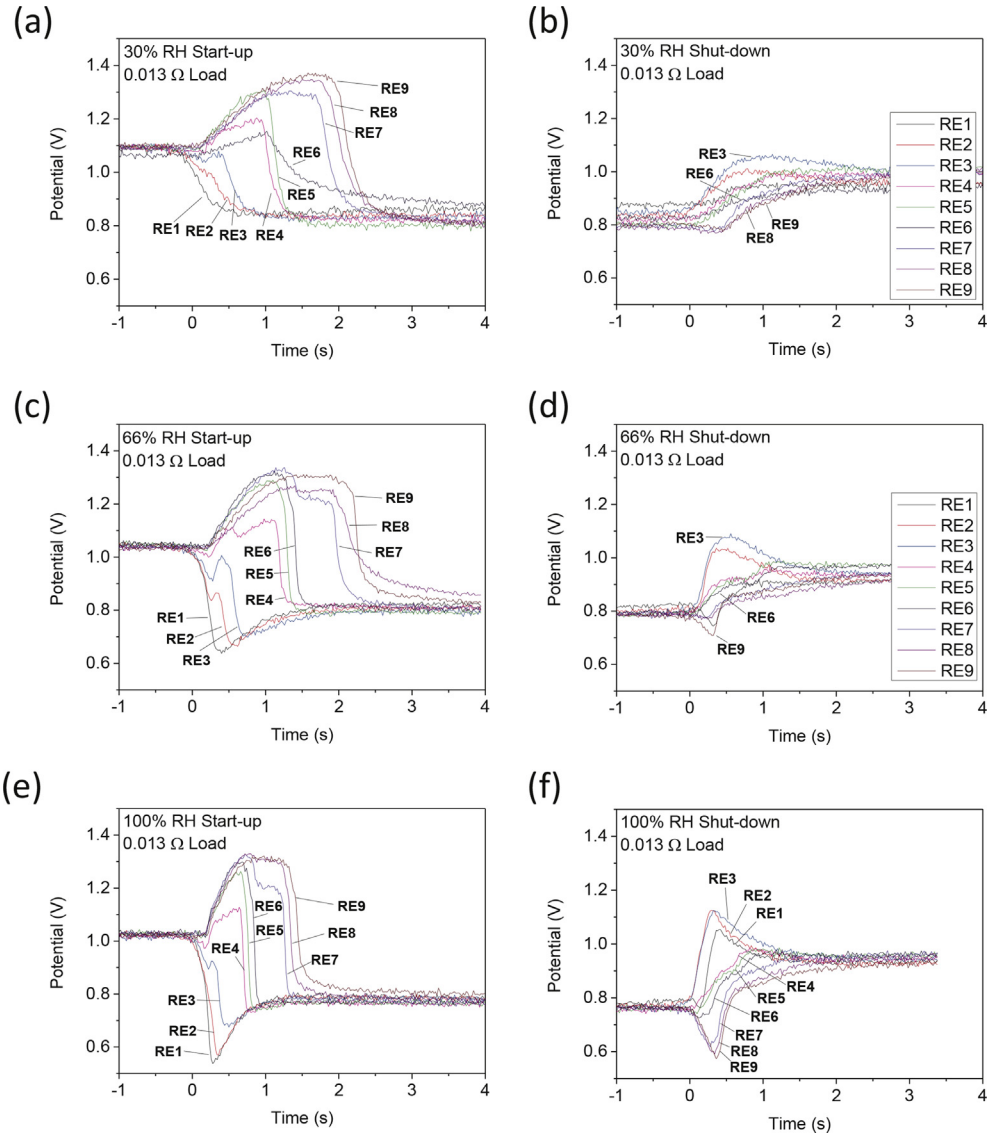

Fig. 8. Cathode potential transients as a function of flow-field location during start-up/shut-down under external load.

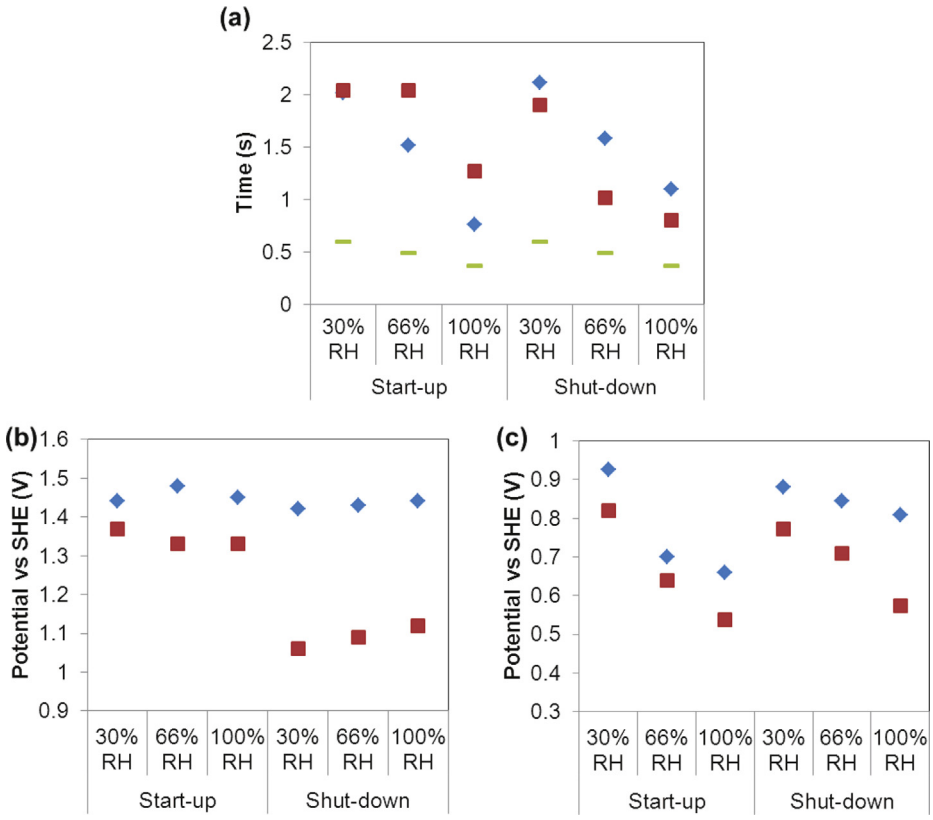

Fig. 9. Summary of cathode potential transient data: (a) duration of the potential spike (b) maximum potential measured during each transient, (c) minimum potential measured during each transient. Blue diamond points represent open circuit measurements; red square points those with an external load. Green lines in figure (a) show calculated gas front residence time in the flow-field (For interpretation of the references to colour in this figure legend, the reader is referred to the web version of this article.).

increasing RH must therefore be linked to ionomer conductivity; it is known that for ionomers such as Nafion, a higher RH leads to a higher proton conductivity, which for a given potential difference across the cell will support a higher carbon corrosion current. As discussed above, flooding of the cathode can disrupt this trend at 100% RH, and the shorter residence time due to humidification may be exacerbating this.

The potential transients yield important information regarding the location and duration of carbon corrosion during SU/SD. Since the duration of the transients does not change appreciably between start-up and shut-down (Fig. 9a), it can be concluded that differences in rates of gas transport between hydrogen and oxygen are not a primary factor in this particular cell. Furthermore, comparison with the CO_2 measurements in Fig. 5 implies that the carbon corrosion current is significantly higher during start-up than during shut-down. This is reflected in the potential transients in Fig. 6, which show that the magnitude and duration of the potential spike is significantly greater in the middle of the flow-field (RE 4–6) during start-up, particularly under wetter conditions. For example, at 100% RH the maximum potential in the middle of the flow-field is about 1.4 V during start-up, compared to around 1.2 V during shut-down. This difference between start-up and shut-down can be ascribed to the influence of platinum hydride/oxide redox kinetics as discussed in Section 2. Opposing effects will occur depending on whether the platinum surface is being reduced (start-up) or oxidised (shut-down) in the region of the anode opposite where the carbon corrosion is occurring (Fig. 1). This difference is evident in the potential transients recorded on the anode in Fig. 10. Potential transients on the anode during start-up at 100% RH are shown in Fig. 10a. A rapid transition from ~1 V to ~0.1 V is evident in Region 1 (RE 1–3) as the hydrogen displaces the air close to the anode inlet. However, for the remaining reference electrodes a shoulder is observed in the potential transients at around 0.7 V, reflecting the influence of the reduction of platinum oxide in Region 2, which is not observed during shut-down.

For the results obtained with the application of an external load, the duration of the potential spike is longer for the start-up transients and shorter for the shut-down transients, compared to open circuit mode (Fig. 9a). This is because during start-up under external load hydrogen entering the anode is rapidly consumed to support the external current, which effectively slows down the progress of the hydrogen front as it travels through the flow-field, leading to a longer start-up transient. During shut-down, when air is introduced to the cell, the hydrogen throughout the anode is

Table 1
Calculated expansion of inlet gas due to humidification.

Relative humidity	Volumetric ratio of water:carrier gas	Humidified volume of 1 L of dry gas	Humidified volume of 1 L of dry gas at 80 °C	Actual flow rate at 0.2 sL min^{-1} set-point (L min^{-1})
30%	0.16	1.16	1.50	0.30
66%	0.45	1.45	1.87	0.37
100%	0.89	1.89	2.44	0.49

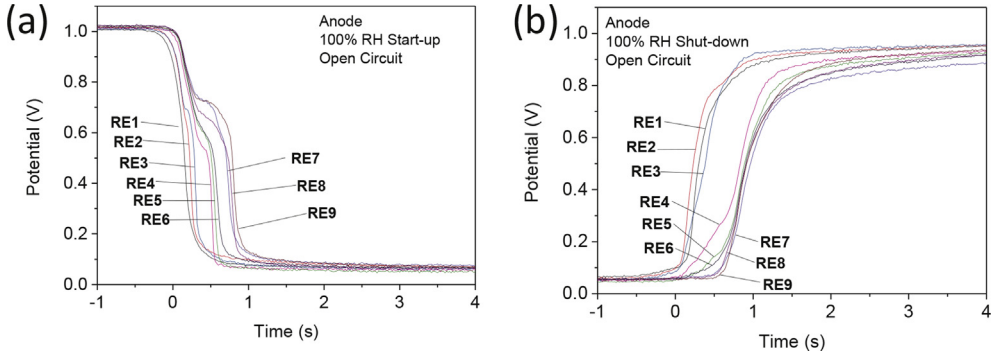

Fig. 10. Anode potential transients during (a) start-up and (b) shut-down at 100% RH.

again being consumed to support the external current and so the driving force for carbon corrosion is depleted faster than it would be by air displacement alone. Therefore the potential transient during shut-down is shorter with an external load than at open circuit. This helps to explain the less effective mitigation of carbon corrosion observed for start-up than for shut-down using external load, although other factors also play a role as discussed above.

The magnitude of the potential spike with an external load is noticeably lower than that at open circuit, most markedly during shut-down (Fig. 9b), which is consistent with the CO_2

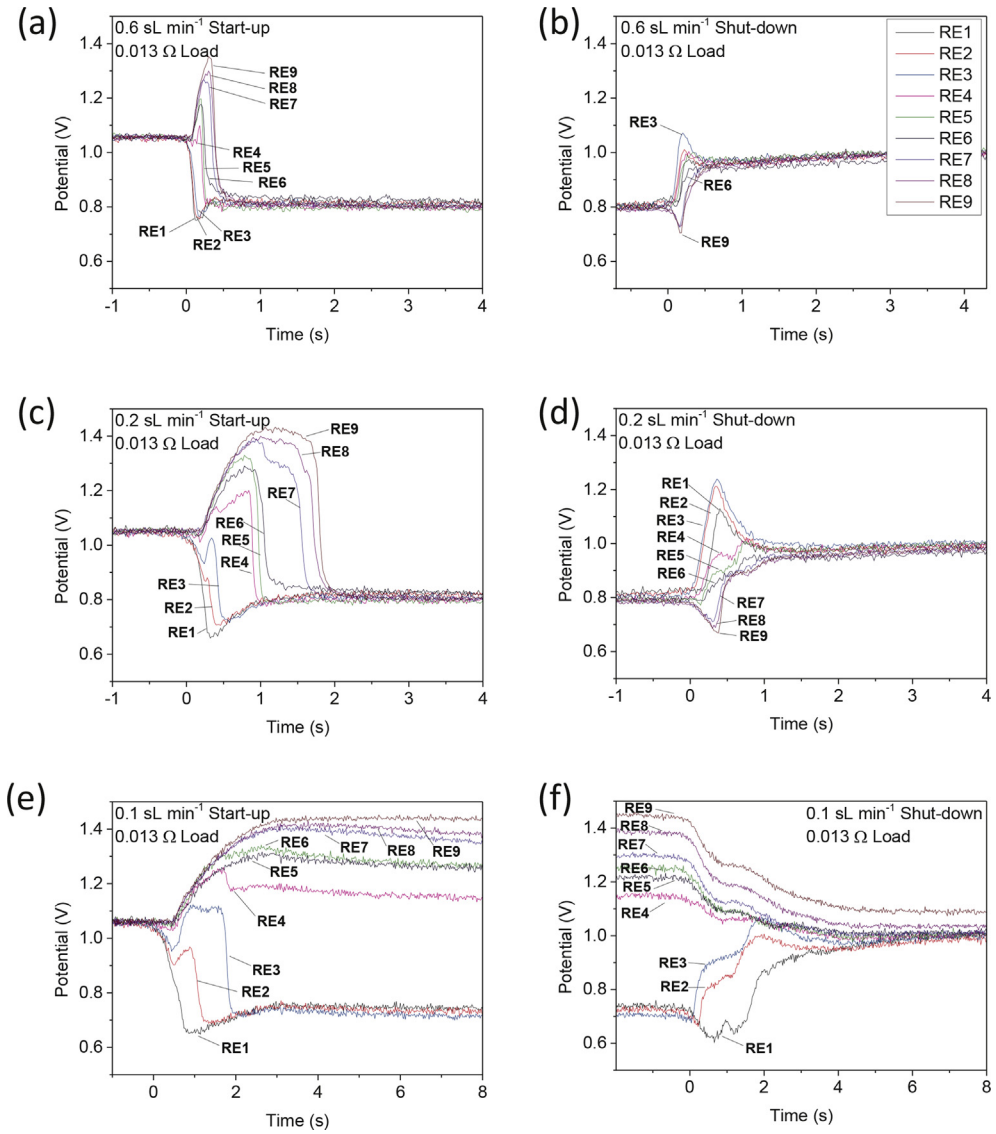

Fig. 11. (a), (c), (e) SU and (b), (d), (f) SD cathode potential transients for (a), (b): 0.6 sL min^{-1}, (c), (d): 0.2 sL min^{-1} and (e), (f): 0.1 sL min^{-1} anode inlet gas flow rates at 66% RH with 0.013 Ω external load.

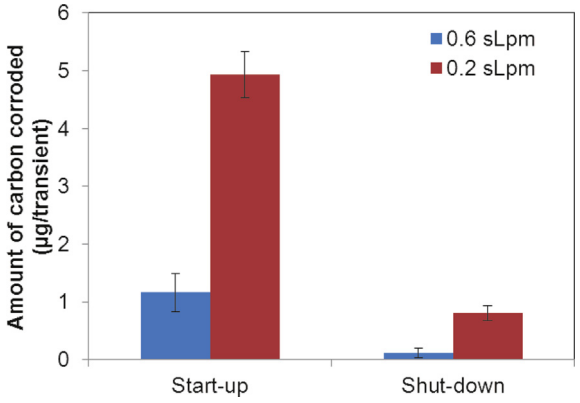

Fig. 12. Calculated amount of carbon corrosion during SU and SD transients for 0.6 sL min^{-1} and 0.2 sL min^{-1} inlet gas flow rates.

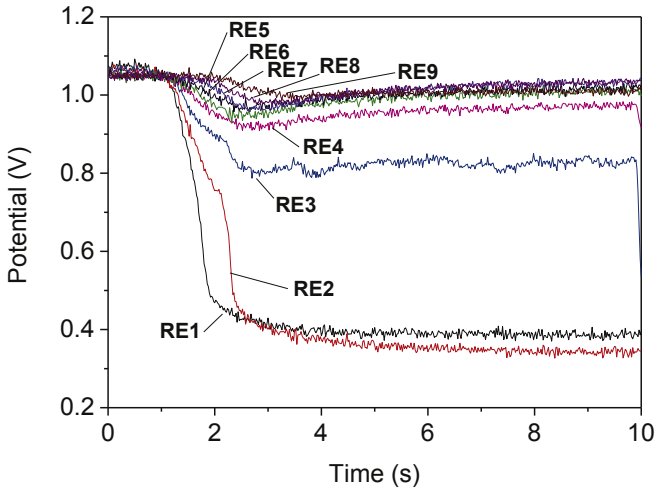

Fig. 14. SU cathode potential transient under external load using constant current mode.

measurements in Fig. 5. The flow of current through the load partially consumes the protons formed in Region 1 (SU) or Region 2 (SD), thus removing some of the driving force for carbon corrosion. No significant effect of RH is evident on the maximum value of the cathode potential during start-up, but a clear increasing trend with RH was observed during shut-down. The minimum potential values observed on the cathode during both start-up and shut-down follow the same trend with RH as those at open circuit, but are more negative (Fig. 9c), reflecting the increased oxygen reduction current drawn by the external load.

4.3. Effect of flow rate

In order to further understand the effect of external load on the progress of the fuel/air front, further SU/SD cycles were carried out on MEA#1 with the application of an external load at 66% RH with varying anode gas flow rates of 0.6 sL min^{-1}, 0.2 sL min^{-1} and 0.1 sL min^{-1}. The potential transients are plotted in Fig. 11, and calculated amounts of carbon corrosion based on CO_2 evolution measurements at flow rates of 0.6 sL min^{-1} and 0.2 sL $min^{-1}$are presented in Fig. 12. From Fig. 11a–d and Fig. 12, it can clearly be seen that as flow rate is increased, and hence the gas front residence time is decreased, both the magnitude and duration of the potential transient are decreased and less carbon corrosion is observed. It can be seen from the potential transients in Fig. 11e and f that at 0.1 sL min^{-1} the cell reaches a steady-state condition whereby the supply of hydrogen at the inlet is entirely consumed by the external current before it reaches RE4, with at least half the cell exposed to elevated potentials continuously until the valve was switched back to shut-down mode after 150 s. Only one cycle at this flow rate was carried out. The CO_2 measurement for this SU/SD cycle is plotted in Fig 13 and shows an initial start-up spike corresponding to corrosion of approx. 6.7 µg of carbon and a smaller shut-down spike corresponding to approx. 0.8 µg of carbon, plus a steady-state carbon corrosion rate of around 0.36 µg s^{-1} throughout the period that hydrogen was supplied. This steady state rate can be converted to a faradaic current of around 12 mA, assuming a 4-electron oxidation of carbon. These carbon corrosion rates are consistent with reports in the literature, which have demonstrated decreases in both electrochemical active area and pore volume of the cathode catalyst layer as a result of SU/SD cycling [14].

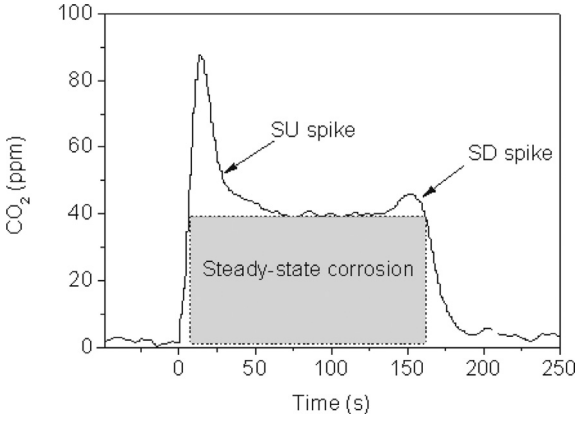

Fig. 13. CO_2 concentration measured in cathode outlet gas during a single SU/SD cycle with anode inlet gas flow rate of 0.1 sL min^{-1}, with 0.013 Ω external load.

This result provides a unique insight into the SU/SD corrosion mechanism. Previously researchers have attempted to simulate the fuel/air boundary inside the cell by using a dual cell configuration connected in parallel [1], however, to our knowledge this is the first time a steady-state condition has been measured in an operating fuel cell. It is interesting to note that even though hydrogen is being consumed by the external load on the cell, there is still a significant carbon corrosion current. In a final experiment, a SU/SD cycle was carried out with the load bank operating in constant current mode, which effectively short-circuited the cell rather than being restricted to the minimum resistance of 0.013 Ω that was available on the hardware in constant resistance mode. At a set-point of 21 A, a measured current of 14.7 A was achieved. This is within experimental error the theoretical maximum current that can be supplied by 0.1 sL min^{-1} of H_2 (14.4 A). In this final cycle, no measurable amount of CO_2 was detected, and the potential transient is shown in Fig. 14. There is no detectable spike in potential, but only the regions of the electrode close to RE1 and RE2 are cathodically polarised, indicating the extent of fuel starvation occurring. We can conclude that in order to achieve satisfactory mitigation of carbon corrosion for start-up, the external resistance must be significantly lower than the internal lateral resistance between the fuel/air and air/air sides of the cell. Of course, in stack applications this technique carries with it a significant risk of cell reversal with potentially more severe implications for cell damage than the SU/SD degradation itself. The NPL reference electrode would be well-suited for a future study in this area.

5. Conclusions

The mechanism of SU/SD degradation in PEMFCs has been investigated using an innovative reference electrode array developed at NPL, which enables in situ mapping of the electrode potential with high time resolution. For the first time, cathode potential mapping has been coupled with simultaneous quantification of carbon corrosion, providing a powerful tool for understanding catalyst support corrosion processes. The reference electrode array pinpoints the location and duration of the carbon corrosion, while the CO_2 measurements provide simultaneous information on the average rate of the corrosion reaction. The results have been discussed in the context of a schematic framework for the reverse current decay mechanism expressed in terms of local electrode potential. This technique could be readily extended to the study of hydrogen starvation and other critical PEMFC degradation modes.

Acknowledgements

This work was supported by the UK National Measurement System under the Innovation R&D Programme and by the EU FP7 H2FC project under Grant Agreement Number 284522. The authors are grateful to S. Zhou for helpful discussions and to Johnson Matthey for supply of MEAs.

References

[1] C.A. Reiser, L. Bregoli, T.W. Patterson, J.S. Yi, J.D. Yang, M.L. Perry, T.D. Jarvi, Electrochem. Solid-State Lett. 8 (2005) A273–A276.
[2] R. Borup, J. Meyers, B. Pivovar, Y.S. Kim, R. Mukundan, N. Garland, D. Myers, M. Wilson, F. Garzon, D. Wood, P. Zelenay, K. More, K. Stroh, T. Zawodzinski, J. Boncella, J.E. McGrath, M. Inaba, K. Miyatake, M. Hori, K. Ota, Z. Ogumi, S. Miyata, A. Nishikata, Z. Siroma, Y. Uchimoto, K. Yasuda, K.-I. Kimijima, N. Iwashita, Chem. Rev. 107 (2007) 3904–3951.
[3] Y. Yu, H. Li, H. Wang, X.-Z. Yuan, G. Wang, M. Pan, J. Power Sources 205 (2012) 10–23.
[4] A. Lamibrac, G. Maranzana, O. Lottin, J. Dillet, J. Mainka, S. Didierjean, A. Thomas, C. Moyne, J. Power Sources 196 (2011) 9451–9458.
[5] N. Linse, G.G. Scherer, A. Wokaun, L. Gubler, J. Power Sources 219 (2012) 240–248.
[6] S. Kreitmeier, A. Wokaun, F.N. Buchi, J. Electrochem. Soc. 159 (2012) F787–F793.
[7] W. Gu, R.N. Carter, P.T. Yu, H.A. Gasteiger, ECS Trans. (2007) 963–973.
[8] Q. Shen, M. Hou, D. Liang, Z. Zhou, X. Li, Z. Shao, B. Yi, J. Power Sources 189 (2009) 1114–1119.
[9] G. Hinds, E. Brightman, Electrochem. Commun. 17 (2012) 26–29.
[10] J. Dillet, A. Lamibrac, G. Maranzana, J. Durst, D. Spernjak, J. Fairweather, R. Mukundan, R.L. Borup, S. Didierjean, O. Lottin, ECS Trans. (2013) 701–710.
[11] P.T. Yu, W. Gu, R. Makharia, F.T. Wagner, H.A. Gasteiger, ECS Trans. (2006) 797–809.
[12] R.T. Atanasoski, D.A. Cullen, G.D. Vernstrom, G.M. Haugen, L.L. Atanasoska, ECS Electrochem. Lett. 2 (2013) F25–F28.
[13] B. Hardy, in: Proceedings of the Third International Symposium on Humidity and Moisture, Teddington, London, England, 1998.
[14] H. Schulenburg, B. Schwanitz, N. Linse, G.G. Scherer, A. Wokaun, J. Phys. Chem. C 115 (2011) 14236–14243.